sciendo
DOI: 10.2478/agriceng-2023-0002

ISSN 2083-1587; e-ISSN 2449-5999
2023,Vol. 27,No.1, pp.11-32
Agricultural Engineering
www.wir.ptir.org

NUMERICAL SIMULATION OF SOIL WATER DYNAMICS IN AUTOMATED DRIP IRRIGATED OKRA FIELD UNDER PLASTIC MULCH

Vidya K. Nagaraju[*a], Karuppalaki Nagarajan[b], Balaji Kannan[c], Subbiah Ramanathan[d], Ramasamy Duraisamy[e]

[a] PhD Scholar, Department of Soil and Water Conservation Engineering, Tamil Nadu Agricultural University, Coimbatore, 641003. Tamil Nadu, India, e-mail: vidyakn45@gmail.com, ORCiD 0000-0002-9037-078X
[b] Faculty of Agricultural Engineering, Department of Soil and Water Conservation Engineering, Tamil Nadu Agricultural University, Coimbatore, 641003. Tamil Nadu, India, India, e-mail: naga_agri@yahoo.com
[c] Faculty of Agricultural Engineering, Department of Soil and Water Conservation Engineering, Tamil Nadu Agricultural University, Coimbatore, 641003. Tamil Nadu, India, India, e-mail: balajikannan73@gmail.com, ORCiD 0000-0003-2330-0893
[d] Faculty of Agricultural Meteorology, Department of Agro Climate Research Centre, Tamil Nadu Agricultural University, Coimbatore, 641003. Tamil Nadu, India, e-mail: ramanathan.sp@tnau.ac.in, ORCiD 0000-0002-5376-3816
[e] Faculty of Agricultural Statistics, Department of Physical Sciences and Information technology, Tamil Nadu Agricultural University, Coimbatore, 641003. Tamil Nadu, India, India, e-mail: mrd7@tnau.ac.in

** Corresponding author: e-mail: vidyakn45@gmail.com*

ARTICLE INFO

Article history:
Received: October 2022
Received in the revised form: November 2022
Accepted: December 2022

Keywords:
Automated drip irrigation,
HYDRUS-2D,
mulch scenario,
rootzone moisture,
soil water movement

ABSTRACT

In India, drip irrigation with plastic mulch is a common practise for irrigation that conserves water. For the design and administration of irrigation regimes, a thorough understanding of the distribution and flow of soil water in the root zone is required. It has been demonstrated that simulation models are effective tools for this purpose. In this work, an automated drip-irrigated Okra field with seven treatments namely T1- Soil moisture-based drip irrigation to 100% FC, T2- Soil moisture-based drip irrigation to 80% FC, T3- Soil moisture-based drip irrigation to 60% FC, T4- Timer based drip irrigation to 100% CWR, T5- Timer based drip irrigation to 80% CWR, T6- Timer based drip irrigation to 60% CWR and T7- Conventional drip irrigation at 100% CWR were utilised to mimic the temporal fluctuations in soil water content using the numerical model HYDRUS-2D. With the help of the observed data, the inverse solution was used to optimise the soil hydraulic parameters. The model was used to forecast soil water content for seven field treatments at optimal conditions. Root mean square error (RMSE) and coefficient of determination (R2) were used to assess the congruences between the predictions and data. With RMSE ranging from 0.036 to 0.067 cm3 cm-3, MAE ranging from 0.020 to 0.059, and R2 ranging from 0.848 to 0.959, the findings showed that the model fairly represented the differences in soil water content at all sites in seven treatments.

Introduction

Globally, agriculture is the major user of fresh water, accounting for over 70% of all global fresh water resources, largely used for crop irrigation. The average agricultural irrigation efficiency worldwide is approximately 50-60% (Lasonya et al., 2016). With water being the critical input for agriculture in nearly all cultivational and growth aspects, it has a determining effect on the eventual crop yield. If plants are not given the right amount of water, even good seeds and fertilisers cannot grow to their full potential. India would have severe water shortages by 2050, according to the OECD Environmental Outlook 2050. Due to rapid ground water depletion and inadequate irrigation infrastructure, 90% of the water consumed in India is used for agriculture (GFFA, 2017). Soil moisture/water content can be monitored and computed directly using watermark sensors, tensiometers, and capacitance probes (Enciso et al., 2007; Thompson et al., 2007). The selection of sensor will depend on soil moisture range to be monitored, price, simplicity to use, and the sensor's performance dependability. According to Mun˜oz-Carpena et al., (2005), granular matrix (GM) sensors and dielectric sensors such as time domain reflectometry (TDR) need less on-site maintenance compared to tensiometers and have a larger likelihood for commercial use. The utilisation of soil moisture data from GM sensors as a decision-making tool for irrigation is straightforward and economical. But the sensor measurement greatly relies on the soil type, weather conditions, plant root zone depth, soil salinity, and soil temperature. The need for calibration, installation requirements, and location restrictions should also be considered when selecting a sensor. Irrigation scheduling based on evapotranspiration methodology varies from simple technique of manually programming the controllers using historical weather data to more intricate methods of using real-time weather data as measured by on-site systems that assess this data and determines the irrigation rate (Kisekka et al., 2010). However, instead, the soil moisture sensing technology uses a soil moisture threshold value that is applied to irrigate depending on the actual measured soil water data. Though, in certain soil types with extremely diverse textures and huge void spaces that existing soil moisture sensor technologies might not measure the exact soil moisture in the fields. The deployment of soil water-based or ET based irrigation scheduling strategies would require training farmers since installation instructions for readily available devices do not always contain the technical knowledge needed to establish the system and instal an automated irrigation method. Simulation models are commonly used to enhance the design, administration, and operation of irrigation systems. Flexibility, cost, analysis, and the examination of numerous scenarios are some of the benefits of employing models. Šimůnek et al., (1999, 2006) created the HYDRUS- 2D model to mimic the two-dimensional flow of water, heat, and solute in a porous media. In drip irrigation systems, determining soil moisture is quite simple and has been a preferred method to evaluate the amount of irrigation water requirement. But, if the water gradients are high, it will be hard to identify the exact location where the soil water content represents and to detect the entire root volume. Although plant-based data presents an efficient technique to plan irrigation and its schedule, the data will not help to determine the amount of water to be supplied. In addition, standardization techniques are necessary to identify operational thresholds (Jones, 2004). To overcome these challenges, convenient tools such as software packages that simulate water transport in the soil-plant-atmosphere (SPA) continuum are often used to evaluate indirectly the soil and crop water status and to estimate indicating parameters related to water stress (Minacapilli et al., 2009; Cammalleri

et al., 2013; Rallo et al., 2017). Many agro-hydrological simulation models have been built and utilised to describe the water transport processes that occurs in the SPA continuum (Rallo et al., 2012). The complexity of the system not only stems from the number of variables to be described, but also from internal self-regulation processes happening across the system components (Rallo et al., 2010). HYDRUS-2D package (Šimůnek et al., 1999) enables modelling water, thermal, and various solute movement in porous media that are variably saturated. Since its development, the model has been widely employed as detailed in the review by Šimůnek et al., (2016). This review covered the capabilities and the primary applications enabled by the various updates and versions of the software were also presented and analysed. Despite the use of this model for determining the water requirement for horticultural crops cultivated in different climatic zones considering the soil moisture content (Ghazouani et al., 2016), only a handful of the studies have included the influence of irrigation strategies on plant water uptake, crop transpiration and/or crop yield (Mailhol et al., 2011). As a response to several research issues, this study investigated alternative irrigation systems, employing basic procedures that would be readily adopted by farmers with minimum support from an irrigation specialist. The application of such technologies is highly current owing to tremendous constraints on water resources, the impending issue of water scarcity being reported globally and the necessity to optimise industrial techniques for economic feasibility. The aim of this thesis work is to compute the effects of executing varying irrigation practices on plant growth and yield parameters. The evaluated systems included automated switching tensiometers for irrigating based on soil water status, irrigating based on evapotranspiration calculated from historical weather data, and the standard schedule irrigation management. In addition, also to examine the efficiency of HYDRUS-2D model to estimate soil water contents to develop effective irrigation system.

Materials and Methods

Weather and climate

The cropping period considered for the study included rainy season of *2021* (sowing date:6th September 2021) and summer season of 2022 (sowing date:21st march 2022), the average maximum and the minimum temperature recorded, ranged from 33.4ºC and 22.5ºC, 32.0ºC and 21.8ºC, respectively. A total rainfall of 453 mm and 102 mm was received during 2021 and 2022, respectively. The average relative humidity ranged from 82.7 and 83.2 percent to 40.4 and 45.0 per cent (14.22 hrs), respectively. The average bright sunshine hours· day^{-1} of 4.5 hours with an evaporation of 4.8 mm·day^{-1} in 2021 *rainy season* and 6.4 hours of sunshine hours·day^{-1} with an evaporation of 6.1 mm·day^{-1} during 2022 *summer season*. The mean wind velocity recorded were 5.6 and 6.5 km·hr^{-1}, respectively.

Experimental Site and Details

The field no NA05 at the eastern block farm, PFDC, TNAU, Coimbatore was used to conduct the experiment. The geographical location of experimental site was in the North-Western agro-climatic zone of Tamil Nadu at 11º 0’ 41” North latitude and 76º 56’23” East longitude which is having altitude of 426.7 m above the mean sea level. The field experiment

consisted of seven main experiments with three replications which were planned in a randomized block design. The trial field possess clay loam textured soil with a pH of 8.44 and an electrical conductivity of 0.62 $dS \cdot m^{-1}$. The soil had 146 $kg \cdot ha^{-1}$ of accessible nitrogen, 49 $kg \cdot ha^{-1}$ of phosphorus, and 1363 $kg \cdot ha^{-1}$ of potassium before the transplant. The experimental site's soil depth was calculated at 40 cm. Soil physical parameters, such as bulk density, particle density, pore space, and infiltration rate, as well as soil moisture constants, such as field capacity and permanent wilting point, were determined. The average value of the sand, silt, and clay percentages in the soil were calculated using the Robinson pipette method in the laboratory. Table.1 lists the precise physio-chemical characteristics of the test area.

Table 1.
Physico-chemical properties of the soil from the experimental field

Soil characteristics	Particulars	Composition
Textural composition	Sand, %	44.50
	Silt, %	19.00
	Clay, %	36.50
	Soil texture	Clay loam
Chemical properties	Available Nitrogen (N), $kg \cdot ha^{-1}$	146.0
	Available Phosphorous (P_2O_5), $kg \cdot ha^{-1}$	49.0
	Available K_2O, $kg \cdot ha^{-1}$	1363
	pH	8.44
	EC, $dS \cdot m^{-1}$	0.62
Physical characters	Bulk density, $g \cdot cc^{-1}$	1.48
	Field capacity, %	27.6
	Permanent wilting point	18.6
	Infiltration rate, $cm \cdot h^{-1}$	1.53

Treatment details

The field experiment treatment was designed to include variations on drip irrigation based on field capacity (FC) and crop water requirement (CWR). A field experiment details are T_1- Soil moisture-based drip irrigation to 100% FC, T_2- Soil moisture-based drip irrigation to 80% FC, T_3- Soil moisture-based drip irrigation to 60% FC, T_4- Timer based drip irrigation to 100% CWR, T_5- Timer based drip irrigation to 80% CWR, T_6- Timer based drip irrigation to 60% CWR and T_7- Conventional drip irrigation at 100% CWR (control). The T_1-T_6 were mulched and irrigated with automated drip irrigation system, T_7 was under no mulch and manual drip irrigation condition. The black plastic mulch was laid to all the treatment excluding control treatment. Mulching was done using 30-micron thickness polythene films. Mulch was laid carefully by providing a cut of 5 cm diameter hole for sowing. In the treatment plots, baseline applications of 50% N, 75% P_2O_5, and 50% K_2O were made from the 100% RDF in the forms of urea, SSP (single super phosphate), and MOP (muriate of potash). In the treatment plots, the final top dressing of 50% N, 25% P_2O_5, and 50% K_2O was applied 30 days after planting (DAP).

Crop Season and variety

Two trial experiments were carried out during th *Rainy* season of 2021 and *Summer* season of 2022. Bhendi crop (variety: COBh H4) was chosen for this study. The spacing adopted was 60x45 cm, the crop duration was 110 days.

Measurement of soil moisture content at root zone

The soil moisture content was measured each day for the entire crop duration in both seasons. Soil samples for gravimetric moisture estimation were collected using a screw auger. Soil samples were taken at 2 points vertically (each at 15 and 30 cm) at the crop root zone in the same location. Since the maximum rootzone was 35 cm, soil variability was not considered. The wet weight (Ww) was determined by oven drying the samples at 105ºC for 24 hours. The measured gravimetric moisture content data was converted into volumetric soil moisture content for calibrating and validating the HYDRUS-2D model. The percent soil moisture content (%) on a dry weight basis was calculated as:

$$\text{Soil moisture content (\%)} = \frac{W_W - D_W}{D_W} \times 100 \quad (1)$$

where:

W_w – the weight of wet soil, (g)
D_w – the weight of dry soil, (g)

HYDRUS-2D model description

A windows-based computer programme called HYDRUS-2D is used to model the two-dimensional movement of water, heat, and solutes in variably saturated flow. With the aid of this computer programme, the Richards equation for saturated and unsaturated water flow can be solved numerically (Dario Autovino et al., 2018). Sink term is taken into account by Richards equation. It reflects the amount of water drained or absorbed by roots. During the water flow simulation, the specified pressure head, flux barriers, atmospheric boundary conditions, no flux boundary, and free drainage boundary conditions were enforced. In a two- or three-dimensional space, the water flow and solute transport can take place in either an axisymmetric or vertical plane.

Model description

The model was used mimic the soil water distribution in a soil profile under various automated drip irrigation systems with various amounts of irrigation treatments. HYDRUS-2D applies the Galerkin finite element method to numerically solve the Richards governing equation for variably saturated water flow (Richards, 1931) under the homogeneous and isotropic soil assumption:

$$\frac{\partial \theta}{\partial t} = \frac{\partial}{\partial x}\left[K(h)\frac{\partial h}{\partial x}\right] + \left[K(h)\frac{\partial h}{\partial z}\right] + \frac{\partial K(h)}{\partial z} - S(h) \quad (2)$$

where:
h – stands for the soil water pressure head, (cm)
K(h) – is the unsaturated hydraulic conductivity, (cm·day^{-1}),
S – is the root water uptake sink term,
Theta – is the volumetric water content of the soil, (cm^3·cm^{-3}),
t – is time, (day)
x and z – are the horizontal and vertical coordinates, respectively, (day^{-1})

Root water uptake

The sink word S_w denotes the amount of water that is absorbed by plants and eliminated from a unit volume of soil during a given period of time. Based on the Feddes et al., (1978) model, the water stress is taken into account.

$$S_w(h) = \alpha(h)S_p \tag{3}$$

where:
S_p – is the potential root water uptake rate, (d^{-1})
h – is the soil water pressure head, (cm)
(h) – is the water stress response function, which ranges from zero to one.

Within the root zone, the potential root water uptake rate is not distributed uniformly:

$$S_p = b(x,z)S_t T_p \tag{4}$$

where:
S_t – is the length of the soil surface associated with transpiration, (cm)
T_p – is the potential transpiration rate,
b (x, z) – is the normalised root water uptake distribution in the vertical x-z plane, (cm^{-2}) (cm-d^{-1}). The following definition applies to the root water uptake distribution b (x, z):

$$b(x,z) = \left(1 - \frac{x}{X_m}\right)\left(1 - \frac{z}{Z_m}\right) e^{-\left(\frac{p_x}{X_m}|x^* - x| + \frac{p_z}{X_m}|z^* - z|\right)} \tag{5}$$

where:
X_m and Z_m – are the maximum width and depth of the root zone (cm) respectively,
x*and z* – the location of the maximum root water uptake in the horizontal and vertical directions respectively. px and pz are the empirical parameters (Vrugt et al., 2001).

Initial conditions

The pressure head's initial spatial distribution was imposed over the flow domain. The dialogue box for the water flow beginning condition displays three choices. A linear distribution with depth, B hydrostatic equilibrium starting from the lowest nodal point, and C the same value at all selected nodes. The initial condition was the observed water distribution in the various soil layers within the flow region.

Boundary conditions

The simulations were run on a 45x50 domain (45 cm is horizontal distance away from the emitter and 50 cm is the depth below the emitter). With the appropriate emitter at the centre, the flux radius is the same as the wetted radius. The conceptual diagram of the simulated area and the enforced boundary constraints is shown in Figure 1 and Figure 2. The bottom and lateral boundaries were regarded as no flux and free drainage zones. The distance between the emitter was 45 cm and 25 cm and was regarded as the variable flux boundary, while the remaining space regarded as the absence of no flux condition for mulched condition and atmospheric boundary condition for no mulched condition.

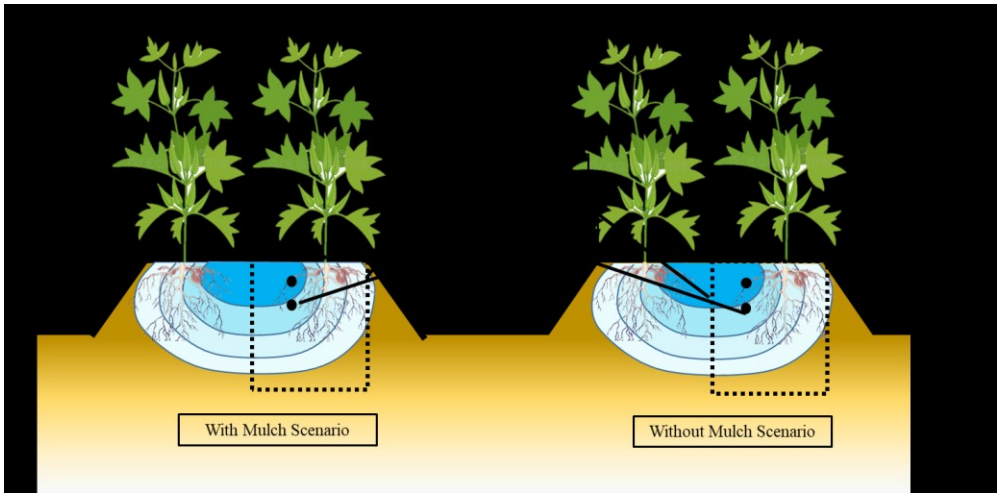

Figure 1. Conceptual diagram of simulated area

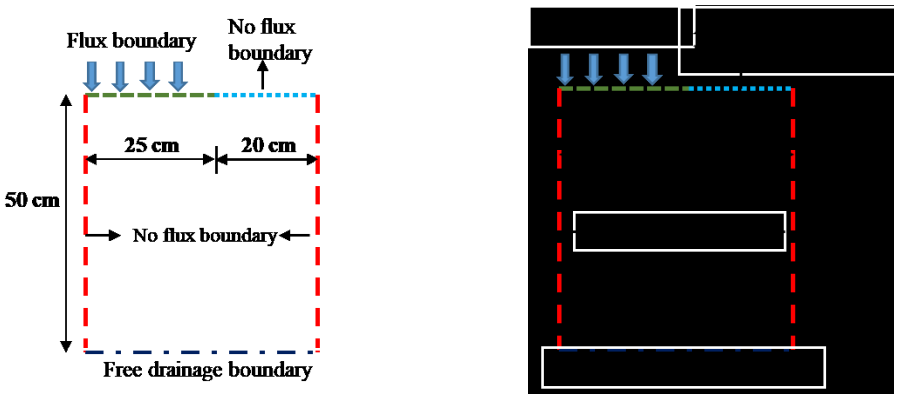

with mulch without mulch

Figure 2. Imposed boundary condition for both scenarios

Input data for HYDRUS

HYDRUS requires potential evaporation and potential transpiration fluxes as input values. Separation of evaporation and transpiration was done by the leaf area index method. The reference crop evapotranspiration (ET_0) values were calculated by the Penman-Monteith method, for the cropping periods (September – December, 2021 and March-July, 2022). Reference evapotranspiration (ETo) was calculated using the FAO Penman-Monteith method (Ritchie, 1972):

$$\mathrm{ETo} = \frac{0.408\Delta(Rn-G)n + \gamma \frac{900}{T+273}\, u_2(\mathrm{es}-\mathrm{ea})}{\Delta+\gamma(1+0.34u_2)} \tag{6}$$

where:

ET_o – is the reference evapotranspiration (mm·day^{-1}), Rn is the net radiation at the crop surface, (MJ·m^{-2} day^{-1})
G – is the soil heat flux density, (MJ·m^{-2} day^{-1})
T – is the mean daily air temperature at 2 m height, (ºC)
u_2 – is the wind speed at 2 m height, (m·s^{-1})
e_s – is the saturation vapour pressure, (kPa)
e_a – is the actual vapour pressure, (kPa)
(e_s – e_a) – Saturation vapour pressure deficit (kPa)

The potential crop evapotranspiration ET_c under typical conditions was calculated using the reference crop evapotranspiration (ET_0) and the crop coefficient K_c (Allen et al., 1998).

$$ET_c = ET_0 x K_c \tag{7}$$

Using Ritchie's (1972) crop leaf area index (LAI), this ET_c is divided into potential evaporation (E_p) and potential transpiration (T_p).

$$E_p = ET_c x\, e^{-K_{gr} x LAI} \tag{8}$$

$$T_p = ET_c - EP \tag{9}$$

where:

Kgr is a global sun radiation extension coefficient. Its value for the bhendi crop was taken to be 0.6 (Phogat et al., 2010). Emitter discharge rate divided by wetted surface area will give constant flux. Flux calculation is as follows (Azad et al., 2018).

$$Constant\ flux\ (cm-d^{-1}), q\ = \frac{Flow\ rate\ (cm^3-d^{-1})}{Ponded\ ares\ (cm^2)} = \frac{Q}{A} = \frac{Q}{2WL} \tag{10}$$

where:

q – is the constant flux, (cm-d^{-1})
Q – is the low rate of an individual emitter, (4 lph or 96000 cm^3-d^{-1}),
W – is the width of ponded zone (25 cm) and
L – is the emitter spacing along the drip line, (40 cm)

$$Constant\ flux\ (cm-d^{-1}), q\ = \frac{96000}{(2x25x40)} =\ 48\ cm-d^{-1} \tag{11}$$

-*HYDRUS-2D model calibration and validation

In general, model calibration is the process of fine-tuning a model for a specific problem by adjusting the input parameters (such as soil hydraulic parameters) and beginning or boundary conditions within the acceptable ranges until the simulated model results closely resemble the observed results. Inverse modelling was used in this thesis project to calibrate the HYDRUS-2D model. For model calibration using inverse modelling, the measured soil water content for ten days in the T_1 plot at a depth of 30 cm was employed as an input parameter. Six parameters are displayed in the water flow parameter window during calibration (Table 1). Rosetta Lite version 1.1 module was used to estimate the initial values for the six parameters. The basic soil information, which included the percentages of sand, silt, clay, and bulk soil density, allowed the model to anticipate the initial estimates. The HYDRUS-2D model simulation inputs were the optimal soil hydraulic parameters that were derived via the calibration of the model. By contrasting the simulated data with the actual data, the model was found to be accurate. The HYDRUS-2D model was validated using the observed data for the second, third, and fourth irrigation cycles at a depth of 30 cm.

Model evaluation

The model performance was evaluated by using the following statistical methods. The calculations were carried out using MS Excel from the average of observed and model predicted values.

Root mean square error (RMSE)

The prediction error, or the discrepancy between the predicted value and the actual value, is exaggerated by this strategy. Calculating the root mean squared error (RMSE) is as follows:

$$\mathrm{RMSE} = \sqrt{\frac{1}{n}\sum_{i=1}^{n}(P_i - O_i)^2} \tag{12}$$

Coefficient of correlation

The linear regression between predicted values and model targets is measured by the coefficient of correlation. The formula for computing the coefficient of correlation (C.C).

$$\mathbf{C.C} = \frac{\boldsymbol{Z\sum PO - (\sum P)(\sum O)}}{\sqrt{\boldsymbol{Z\,(\sum P^2) - (\sum P)^2}}\sqrt{\boldsymbol{Z\,(\sum O^2) - (\sum O)^2}}} \tag{13}$$

Mean absolute error

A measurement of the difference between two continuous variables is the mean absolute error. The following equation can be used to get the mean absolute error:

$$MAE = \frac{1}{n}\sum_{i=1}^{n}|P_i - O_i| \tag{14}$$

Results and Discussion

Calibration HYDRUS-2D

Ten days observed moisture content data of T_1 was used for the model calibration. Once the optimization was completed successfully, HYDRUS generates a set of simulated data for the observed moisture data. The comparison of observed and simulated data is generally termed as residual analysis. After evaluation of the uniqueness of an inverse solution by residual analysis, the next logical step is to compare the simulated results with the corresponding field observations. Figure 3 shows the field observed data and corresponding simulated data obtained at different time steps. There exists a best fit between the observed and simulated soil moisture data with a C.C value of 0.892. The optimised values are estimated by l fixed at 0.5, the average value across all soil types. The findings show that when the pore connectivity value was set to 0.5, all the parameters showed a marginally perceptible shift from the initial estimations (Radcliff and Simunek, 2018). In addition, the values of the model evaluation indicators in simulating soil water content using optimized parameter values are presented in Table 2. The optimum values of the parameters are within the common ranges reported in previous studies (Ebrahimian et al., 2013; Ranjbar et al., 2019). The values of and other evaluation indicators for the calibration stage are reasonable. The root mean square error value signifies the difference between observed and simulated value, it was found as 0.034 cm cm^{-1} also correlation coefficient signifies the degree of association between observed and simulated values, it was found as 0.892. Moreover, these values were comparable to the results obtained by Skaggs et al. (2004) and Kandelous et al. (2011). Therefore, it can be concluded that the accuracy of the simulations for different depths of soil layers was satisfactory and that the HYDRUS-2D model can reflect the dynamic changes in soil water at different depths. Hence the model can be used to simulate the soil moisture content for the study domain.

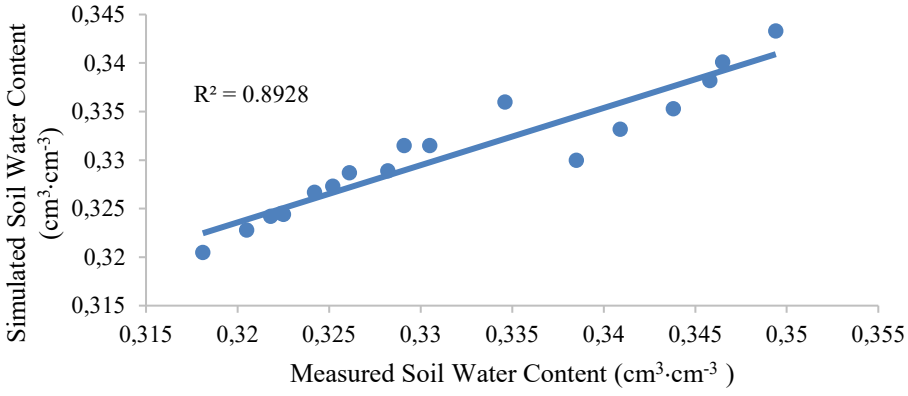

Figure 3. Simulated and measured moisture content of T1 for 10 days

Table 2.
Initial estimates for soil hydraulic parameters for clay loam texture

Parameters	Initial estimates (as per Rosetta lite v. 1. 1)
Residual water content, θ_r ($cm^3 \cdot cm^{-3}$)	0.079
Saturated water content, θ_s ($cm^3 \cdot cm^{-3}$)	0.442
Inverse of the air entry value α, (cm^{-1})	0.016
Parameter n in the soil water retention function	1.414
Saturated hydraulic conductivity K_s, ($cm \cdot min^{-1}$)	0.0568

Validation of HYDRUS-2D

Figure 4 shows the simulated and the observed soil moisture distribution at the end of the simulation period for T_1-T_7 for two seasons at a depth of 30 cm. It was noted that the simulated wetting pattern was in a very close agreement with the observed data. No significant difference was noted between the simulated and observed soil water distributions. The depths and widths of the wetted regions were approximately similar as was the spatial distribution of the water content. To evaluate the performance of HYDRUS-2D model in simulating water distribution within the flow domain, the RMSE, MAE and C.C values between the simulated and the observed data were calculated. Table 3 demonstrates the RMSE, MAE and C.C values for different irrigation treatments and regimes for both seasons. In general, based on RMSE, MAE and C.C values showed good agreement with simulated and measured soil moisture content. The model thus correctly simulated soil water distribution within the soil domain.

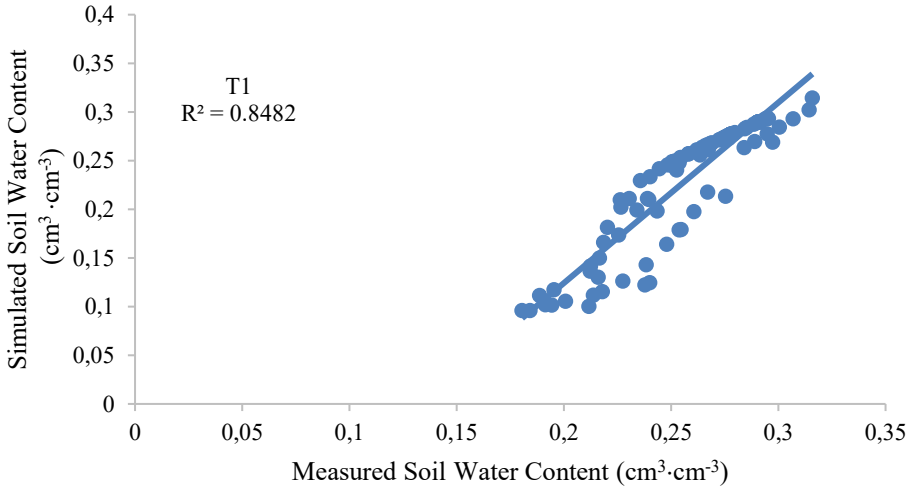

(a)

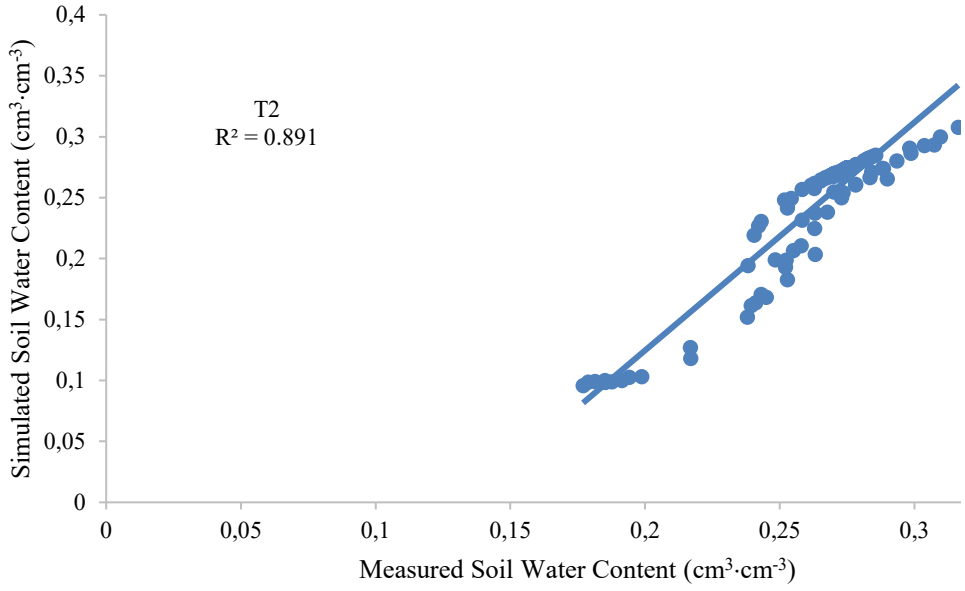
T2
R² = 0.891
Simulated Soil Water Content (cm³·cm⁻³)
Measured Soil Water Content (cm³·cm⁻³)
0
0,05
0,1
0,15
0,2
0,25
0,3
0,35
0,4

(b)

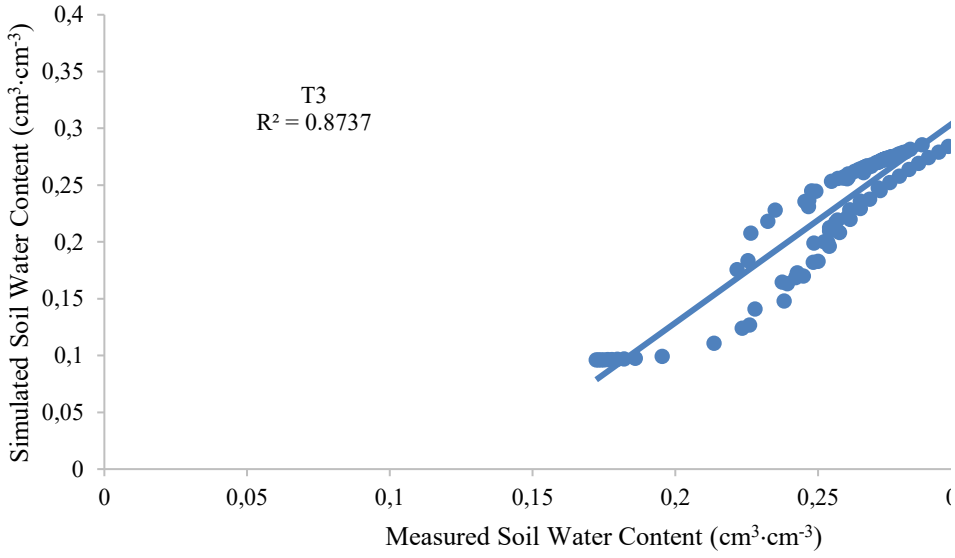
T3
R² = 0.8737
Simulated Soil Water Content (cm³·cm⁻³)
Measured Soil Water Content (cm³·cm⁻³)
0
0,05
0,1
0,15
0,2
0,25
0,3
0,35
0,4

(c)

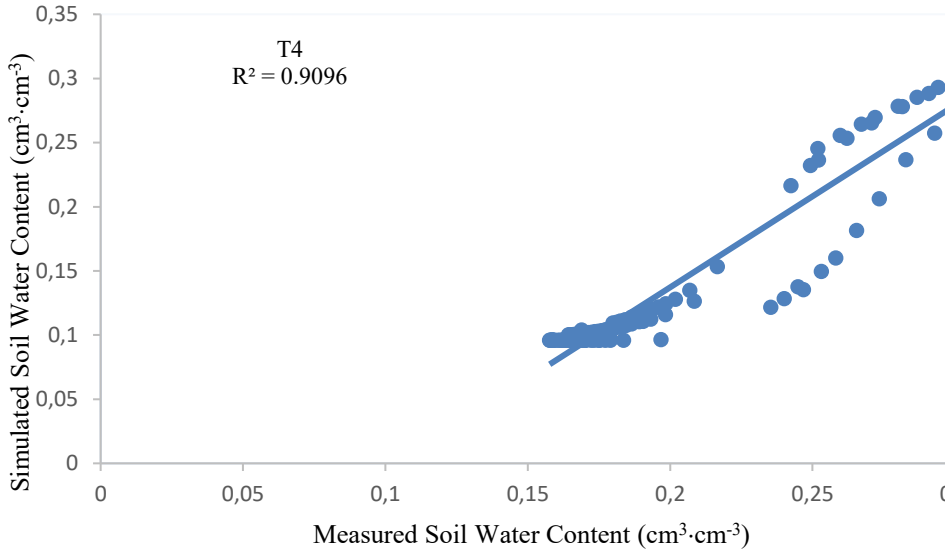
T4
R² = 0.9096
Simulated Soil Water Content (cm³·cm⁻³)
Measured Soil Water Content (cm³·cm⁻³)
0,35
0,3
0,25
0,2
0,15
0,1
0,05
0
0
0,05
0,1
0,15
0,2
0,25

(d)

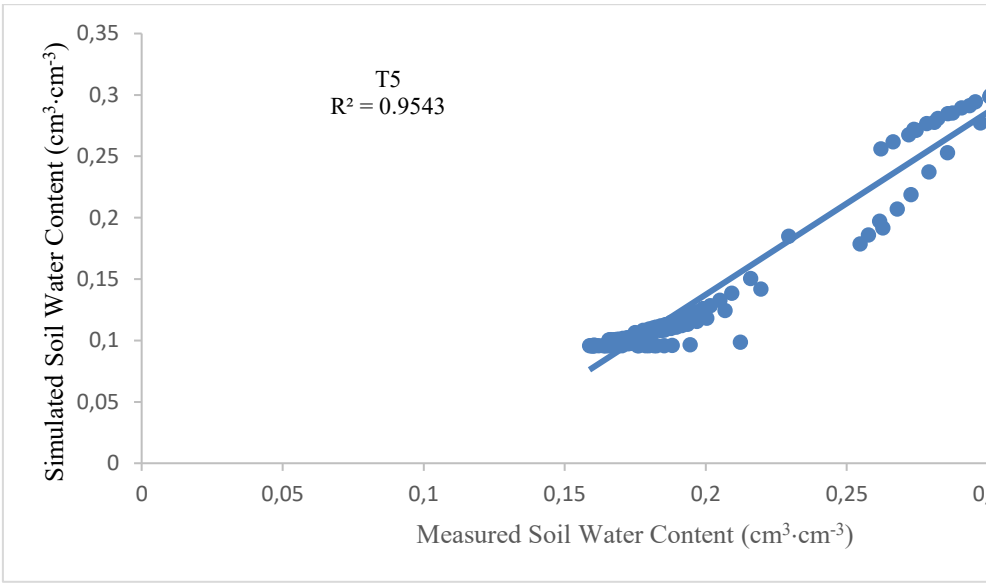
T5
R² = 0.9543
Simulated Soil Water Content (cm³·cm⁻³)
Measured Soil Water Content (cm³·cm⁻³)
0,35
0,3
0,25
0,2
0,15
0,1
0,05
0
0
0,05
0,1
0,15
0,2
0,25

(e)

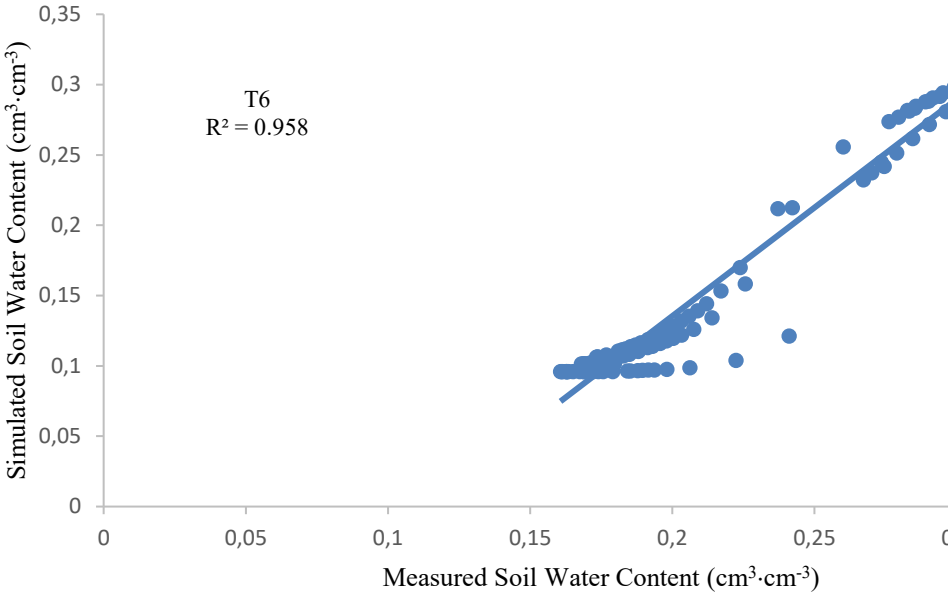
T6
R² = 0.958
Simulated Soil Water Content (cm³·cm⁻³)
Measured Soil Water Content (cm³·cm⁻³)
0,35
0,3
0,25
0,2
0,15
0,1
0,05
0
0
0,05
0,1
0,15
0,2
0,25

(f)

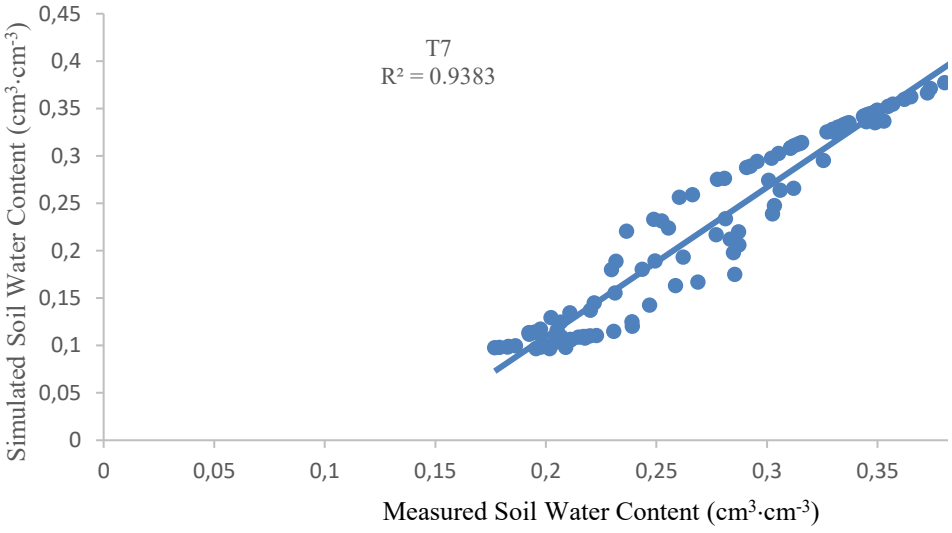
T7
R² = 0.9383
Simulated Soil Water Content (cm³·cm⁻³)
Measured Soil Water Content (cm³·cm⁻³)
0,45
0,4
0,35
0,3
0,25
0,2
0,15
0,1
0,05
0
0
0,05
0,1
0,15
0,2
0,25
0,3
0,35

(g)

Figure 4(a-g). Comparison of the simulated and observed soil water contents of the seven treatments.

Table 3.
Initial and Final estimates of soil hydraulic properties

Parameters	Initial estimates	Final estimates
Residual water content, θ_r ($cm^3 \cdot cm^{-3}$)	0.095	0.0395
Saturated water content, θ_s ($cm3 \cdot cm^{-3}$)	0.442	0.226
Inverse of the air entry value α, (cm^{-1})	0.019	0.010
Parameter n in the soil water retention function	1.31	1.118
Saturated hydraulic conductivity K_s, ($cm \cdot day^{-1}$)	6.24	5.23
Pore connectivity factor, l	0.500	0.500

Table 4.
Comparative statistics for observed and simulated soil water contents

Parameter	T_1	T_2	T_3	T_4	T_5	T_6	T_7
RMSE ($cm^3 \cdot cm^{-3}$)	0.042	0.036	0.041	0.067	0.064	0.064	0.061
MAE	0.023	0.020	0.026	0.059	0.057	0.056	0.044
C.C	0.848	0.891	0.873	0.909	0.954	0.958	0.938

Comparison of Water Distribution Patterns among Treatments

To understand the soil water movement in all the treatments, moisture simulation was carried out for all the seven treatments using HYDRUS 2D model. The simulation of soil moisture was conducted for the single irrigation event at the end of the initial stages of crop for all the seven treatments is discussed in this section. As reported in previous section T_1-T_3 was irrigated based on three levels of field capacity. The flux applied in T_1 was higher compared to the T_2 and T_3. The Figure 5. illustrates that the wetting patterns during the application of water can be mainly categorized into three zones: a saturated zone close to the dripper was represented by blue colour (water content nearly 0.349), a low water–content region located at the right upper corner of the domain indicated by red colour (water content nearly 0.313), and a zone between them represented with different colour variations. A fan-shaped wetting pattern was observed from moisture movement. Irrigation amount, soil properties, and evapotranspiration govern the spatial distribution of water. The radius of the wetting pattern changed dynamically and decreased as the irrigation amount was reduced from T_1 to T_3. For T_1, next irrigation flux was applied after the fourth day, once the moisture content at the root zone reduced to predetermined level. Once the moisture content near the rootzone reduced to 0.333 to 0.313 automated irrigation system was activated to supply next irrigation. Meanwhile, low water content indicated by red colour caused by evapotranspiration was increased as the days increased from the irrigation. T_2 and T_3 are also followed the same pattern of moisture distribution. The major difference observed was irrigation interval. Irrigation interval directly varies with flux applied. Since T_3 was supplied with very less amount of irrigation

water, the moisture content at the rootzone was reduced to the extent to receive next irrigation in the next day. Same way the flux in T_2 was higher than T_3 and lower than T_1, hence irrigation interval was recorded as 2 days. The T_4-T_7 were also irrigated with automated irrigation system, unlike previous treatments, the system worked based on timer based automated scheduling techniques. Figure 5 demonstrates the variation in moisture distribution based on flux applied. In the case of T_4, applied flux was higher and satisfies 100% of crop water requirement. The moisture content at the rootzone immediately after irrigation was observed as 0.330 to 0.333. The root water uptake, evapotranspiration, and percolation of water beyond the rootzone reduces moisture content to 0.317 within three days. In the same way the T_5 satisfies 80% of crop water requirement and reaches 0.317 moisture content range of rootzone moisture within next day of irrigation. This variation was mainly due to the reduction in the flux applied. T_6 was supplied with lowest flux that satisfies only 60% of crop water requirement. The T_7 was irrigated with same flux as T_4, to exhibit the moisture pattern variation under mulch and no mulch condition. Observed two fan shaped pattern, one was near dripper having high moisture content at surface and gradually lowers as soil depth increases. The other was right side of the domain, shows less moisture content at the surface and gradually increase as the soil depth increases. The water content in the deep layers of the soil profiles was relatively stable. It could be concluded that the model could give good soil water distribution simulation results and could reflect the impact of irrigation amounts on soil water distribution and soil water content.

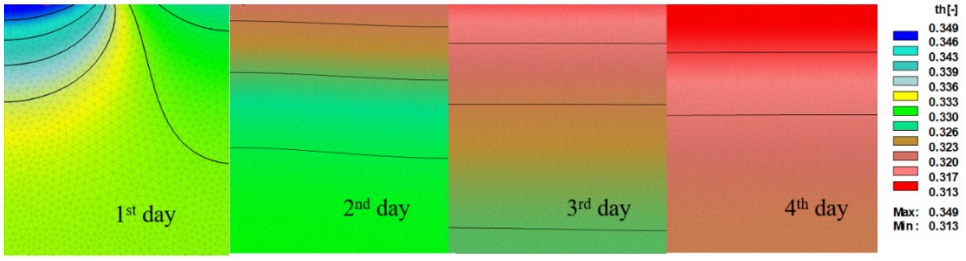

a. T_1

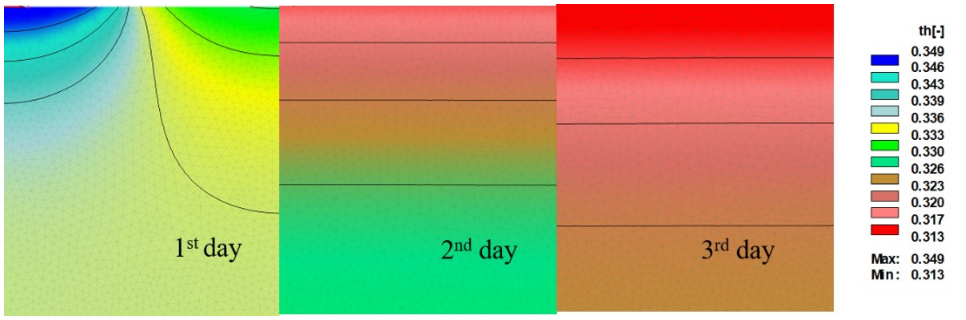

b. T_2

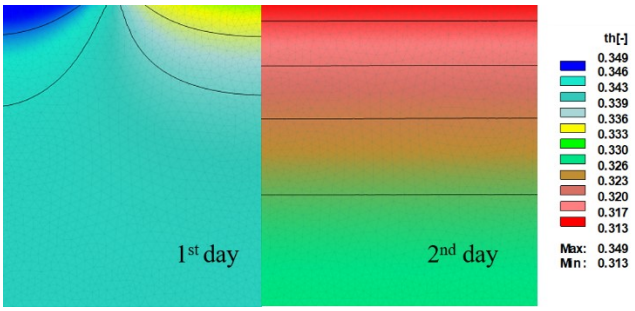
th[-]
0.349
0.346
0.343
0.339
0.336
0.333
0.330
0.326
0.323
0.320
0.317
0.313
Max: 0.349
Min: 0.313
1st day
2nd day

c. T_3

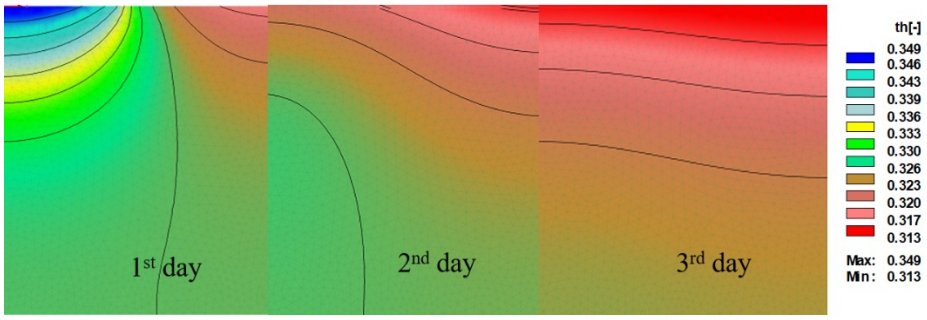
th[-]
0.349
0.346
0.343
0.339
0.336
0.333
0.330
0.326
0.323
0.320
0.317
0.313
Max: 0.349
Min: 0.313
1st day
2nd day
3rd day

d. T_4

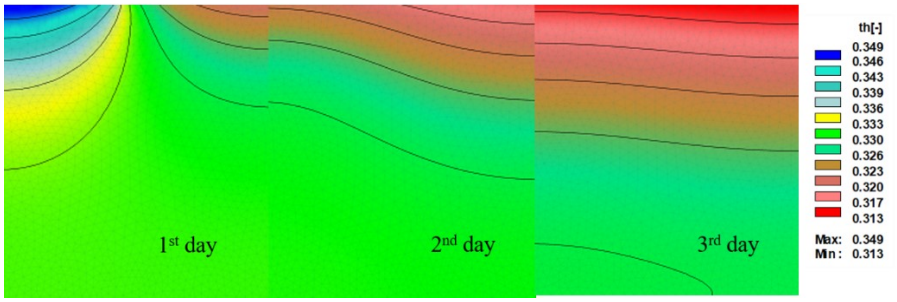
th[-]
0.349
0.346
0.343
0.339
0.336
0.333
0.330
0.326
0.323
0.320
0.317
0.313
Max: 0.349
Min: 0.313
1st day
2nd day
3rd day

e. T_5

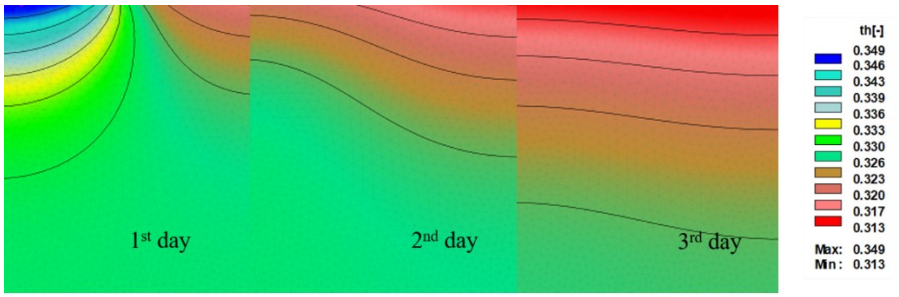

f. T_6

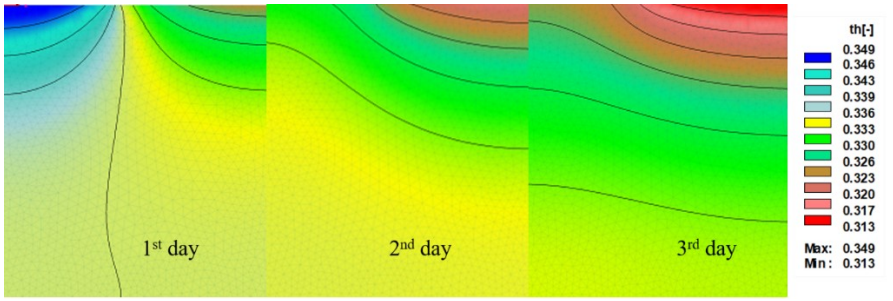

g. T_7

Figure 5 (a-g). Soil moisture distribution pattern for single irrigation event

Effect of Mulch on Soil Water Fluctuation Patterns

The further study concentrates on examination of the effects of mulch on soil water movement under automated drip irrigation and conventional drip irrigation. The automated drip irrigation with 100% CWR (T_6) and conventional drip irrigation with 100% CWR (T_7) are used to study with mulch and no mulch scenarios. In these additional simulations, the scenario with mulch (SM) maintained the same model setup that was described earlier. Compared with SM, the scenario without mulch (SWM) changed the no-flux boundary in the upper domain to the atmosphere boundary conditions. Five days moisture variation was simulated with HYDRUS model for two irrigation flux. The spatial variation of moisture content with represented in the Figure 6 clearly infer that the under-mulch condition moisture movement was vertical. On the first day, the moisture near the root zone varied between 0.330 to 0.333 $cm^3 \cdot cm^{-3}$ and near the upper no flux area was not supplied any moisture. However, that portion was also having moisture range of 0.320 to 0.323 $cm^3 \cdot cm^{-3}$, since it was covered with mulch. It was also found that in the under-mulch scenario, majority of the soil moisture was effectively utilized by the crop. There was no lateral movement of moisture in all the five days simulation. The second irrigation flux applied on 4th day also clearly pictures the absence of evaporation losses in the domain. In this simulation, only a transpiration component was considered for the study duration. Under no mulch scenario the moisture movement was in contrast to mulch scenario. The upper no flux boundary was changed to atmospheric

boundary condition. The evaporation and transpiration components are transferring moisture to the atmosphere. From Figure 6 it was spatially demonstrated that moisture movement was more lateral and also variation in moisture ranges towards the other side of the crop was observed. The moisture movement below the root zone also varied between 0.0342 to 0.0346 cm^3 cm^{-3} on the first day. The moisture near the rootzone was less than the observed moisture with mulch scenario. As the time increases the simulation made clear point that the more water losses due to evaporation and dep percolation. On the fifth day of moisture simulation, large variation moisture movement was observed away from the effective rootzone. Finally, from the study it was clear that covering crop rows with plastic mulch have great influence on efficient utilization crop water for the growth. With mulch application, moisture was saved for the longer duration of crop. The author Ming Han et al., (2015) also studied the moisture movement with mulch and no mulch scenarios. This study significantly showed reduction of evaporation and increased root water uptake. LIU Mei-Xian et al., (2013) indicating that the plastic mulch could prevent about 93% of soil water evaporation.

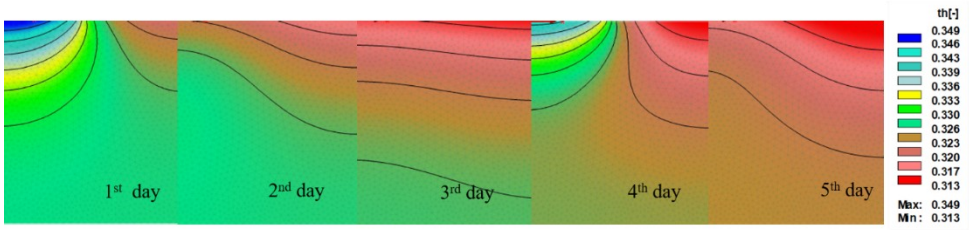

a. With mulch Scenario

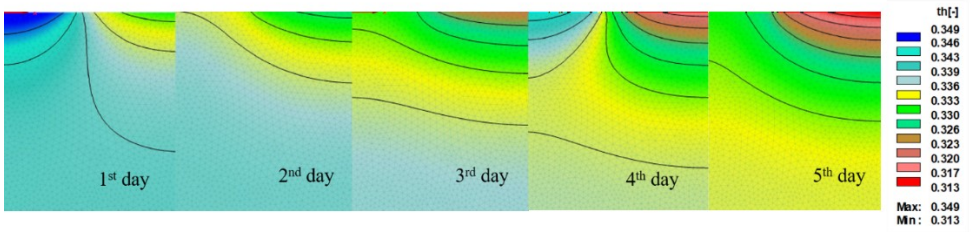

b. Without mulch Scenario

Figure 6. Spatial soil water content distribution under both scenario

Conclusion

The design and maintenance of drip irrigation systems need a thorough understanding of water distribution and movement in the root zone. Field experiments are time-consuming and labour-intensive, and they yield only a small amount of data. Using sparse field data, modelling is a way for acquiring more accurate data. To learn more about the mechanisms governing the distribution of soil moisture and the transportation of soil water, field experiments and modelling techniques are utilised. Field irrigation experiments with four treatments were

carried out for this study. This study's goal was to assess how well the model for replicating the dynamics of soil water under mulch drip irrigation performed. Additional numerical experiments were conducted for this purpose. Okra field irrigated by an automated drip irrigation system with mulch cover used as the testing domain, validation, and application site for the simulation model (HYDRUS-2D). The findings imply that there is considerable agreement between the measured soil water content and the simulated outcomes from HYDRUS-2D. As the administered irrigation was reduced, so were root water absorption, evaporation, and the radius of the wetting zone. To make up for the disparity in irrigation, soil water storage and recharge from low soil profiles were enhanced. According to the simulation's findings, mulch has little impact on how soil water is distributed. Mulch is useful for conserving soil water in the rootzone. It is a common irrigation technique that can minimise evaporation, increase water usage effectiveness, and preserve water in severely dry areas with drip. The HYDRUS-2D model may be used to help with planning and creation of management strategies for drip irrigation systems covered in mulch.

References

Allen, R. G., Pereira, L. S., Raes, D., and Smith, M. (1998). Crop evapotranspiration-Guidelines for computing crop water requirements-FAO Irrigation and drainage paper 56. Fao, Rome, *300*(9), D05109.

Autovino, D., Rallo, G., and Provenzano, G. (2018). Predicting soil and plant water status dynamic in olive orchards under different irrigation systems with Hydrus-2D: Model performance and scenario analysis. *Agricultural water management, 203,* 225-235.

Azad, N., Behmanesh, J., Rezaverdinejad, V., Abbasi, F., and Navabian, M. (2018). Developing an optimization model in drip fertigation management to consider environmental issues and supply plant requirements. *Agricultural water management, 208,* 344-356.

Cammalleri, C., Rallo, G., Agnese, C., Ciraolo, G., Minacapilli, M. and Provenzano, G. (2013). Combined use of eddy covariance and sap flow techniques for partition of ET fluxes and water stress assessment in an irrigated olive orchard. *Agricultural Water Management, 120*, 89-97. http://dx.doi.org/10.1016/j.agwat.2012.10.003.

Dhawan, V. (2017). *Water and agriculture in India: background paper for the South Asia expert panel during the Global Forum for Food and Agriculture (GFFA).* Hamburg, OAV – German Asia-Pacific Business Association.

Ebrahimian, H., Liaghat, A., Parsinejad, M., Playán, E., Abbasi, F., and Navabian, M. (2013). Simulation of 1D surface and 2D subsurface water flow and nitrate transport in alternate and conventional furrow fertigation. *Irrigation Science, 31*(3), 301-316.

Enciso, J.M., Jifon, J., and Wiedenfeld, B. (2007). Subsurface drip irrigation of onions: effects of drip tape emitter spacing on yield and quality. *Agricultural Water Management 92(3)*, 1-7.

Feddes, R.A. (1982). Simulation of field water use and crop yield. In *Simulation of plant growth and crop production.* Pudoc, pp. 194-209.

Ghazouani, H., Autovino, D., Rallo, G., Douh, B., and Provenzano, G. (2016). Using Hydrus-2D model to assess the optimal drip lateral depth for Eggplant crop in a sandy loam soil of central Tunisia. *Italian Journal of Agrometeorology*, *1*, 47-58.

Han, M., Zhao, C., Šimůnek, J., and Feng, G. (2015). Evaluating the impact of groundwater on cotton growth and root zone water balance using Hydrus-1D coupled with a crop growth model. *Agricultural Water Management, 160*, 64-75.

Jones, H.G. (2004). Irrigation scheduling: advantages and pitfalls of plant-based methods. *Journal of experimental botany, 55*(407), 2427-2436.

Kandelous, M. M., Šimůnek, J., Van Genuchten, M. T., and Malek, K. (2011). Soil water content distributions between two emitters of a subsurface drip irrigation system. *Soil Science Society of America Journal, 75*(2), 488-497.

Kisekka, I., Migliaccio, K.W., Dukes, M.D., Schaffer, B., and Crane, J.H. (2010). Real-timeevapotranspiration-based irrigation scheduling and physiological response in a carambola (Averhoha carambola) orchard. *Applied Engineering in Agriculture, 26*(3), 373-380.

Lozoya, C., Mendoza, C., Aguilar, A., Román, A., and Castelló, R. (2016). Sensor-based model driven control strategy for precision irrigation. *Journal of Sensors,* 9784071.

Mailhol, J.C., Ruelle, P., Walser, S., Schütze, N., and Dejean, C. (2011). Analysis of AET and yield predictions under surface and buried drip irrigation systems using the Crop Model PILOTE and Hydrus-2D. A*gricultural Water Management, 98,* 1033-1044.

Mei-Xian, L.I.U., Jing-Song, Y.A.N.G., Xiao-Ming, L.I., Mei, Y.U., and Jin, W.A.N.G. (2013). Numerical simulation of soil water dynamics in a drip irrigated cotton field under plastic mulch. *Pedosphere, 23*(5), 620-635.

Minacapilli, M., Agnese, C., Blanda, F., Cammalleri, C., Ciraolo, G., D'Urso, G., Iovino, M., Pumo, D., Provenzano, G., and Rallo, G. (2009). Estimation of actual evapotranspiration of Mediterranean perennial crops by means of remote-sensing based surface energy balance models. *Hydrology and Earth System Sciences*, *13*(7), 1061-1074.

Mun˜oz-Carpena, R., Dukes, M.D., Li, Y., and Klassen, W. (2005). Field comparison of tensiometer and granular matrix sensor automatic drip irrigation on tomato. *HortTechnology, 15* (3), 584–590.

Radcliffe, D. E., and Simunek, J. (2018). *Soil physics with HYDRUS: Modeling and applications*. CRC press.

Rallo, G., Agnese, C., Blanda, F., Minacapilli, M., and Provenzano, G. (2010). Agro- Hydrological models to schedule irrigation of Mediterranean tree crops. *Italian Journal of Agrometeorology*, 1, 11-21.

Rallo, G., Agnese, C., Minacapilli, M., and Provenzano, G. (2012). Comparison of SWAP and FAO agro-hydrological models to schedule irrigation of wine grape. *Journal of Irrigation and Drainage Engineering*, 138(1).

Rallo, G., González-Altozano, P., Manzano-Juárez, J., and Provenzano, G. (2017). Using field measurements and FAO-56 model to assess the eco-physiological response of citrus orchards under regulated deficit irrigation. *Agricultural water management, 180*, 136-147.

Ranjbar, A., Rahimikhoob, A., Ebrahimian, H., and Varavipour, M. (2019). Simulation of nitrogen uptake and distribution under furrows and ridges during the maize growth period using HYDRUS-2D. *Irrigation Science, 37*(4), 495-509.

Richards, L.A. (1931). Capillary conduction of liquids through porous mediums. *Physics, 1,* 318-333.

Ritchie, J.T. (1972). A model for predicting evaporation from a row crop with incomplete cover. *Water research*, 8, 1204-1213.

Šimůnek, J., Šejna, M., and van Genuchten, M.Th. (1999). The Hydrus-2D Software Package for Simulating Two-dimensional Movement of Water, Heat, and Multiple Solutes in Variably Saturated Media. Version 2.0, IGWMC − TPS − 53. *International Ground Water Modeling Center, Colorado School of Mines Golden*, Colorado 251pp.

Šimůnek, J., Šejna, M., and van Genuchten, M.Th. (2016). Recent developments and applicationsof the Hydrus computer software packages. *Vadose Zone Journal*, 1-25.

Skaggs, T.H., Trout, T.J., Šimůnek, J., and Shouse, P. J. (2004). Comparison of HYDRUS-2D simulations of drip irrigation with experimental observations. *Journal of irrigation and drainage engineering*, *130*(4), 304-310.

Thompson, R.B., Gallardo, M., Valdez, L.C., and Fernandez, M.D. (2007). Determination of lower limits for irrigation management using in situ assessments of apparent crop water uptake made with volumetric soil water content sensors. *Agricultural Water Management 92,* 13-28.

Vrugt, J. A., Hopmans, J. W., and Šimunek, J. (2001). Calibration of a two-dimensional root water uptake model. *Soil Science Society of America Journal, 65*(4), 1027-1037.

SYMULACJA NUMERYCZNA DYNAMIKI WODNEJ GLEBY NA POLU OKRY NAWADNIANYM AUTOMATYCZNYM SYSTEMEM KROPELKOWYM POD FOLIĄ

Streszczenie. W Indiach, nawadnianie kropelkowe pod folią jest popularną praktyką oszczędzania wody. Projekty i zarządzanie systemami nawadniania wymagają zrozumienia rozmieszczenia i przepływu wody glebowej w strefie korzeniowej. Udowodniono, że skutecznym narzędziem do tego są modele symulacyjne. W niniejszej pracy wykorzystano pole okry nawadnianej automatycznym systemem kropelkowym, które podlegało siedmiu zabiegom, mianowicie: T_1 - nawadnianie kropelkowe do 100% pojemności polowej opartej na wilgotności gleby, T_2 - nawadnianie kropelkowe do 80% pojemności polowej opartej na wilgotności gleby, T_3 - nawadnianie kropelkowe do 60% pojemności polowej opartej na wilgotności gleby, T_4 - nawadnianie kropelkowe oparte na czasomierzu do 100% CWR, T_5 - nawadnianie kropelkowe oparte na czasomierzu do 80% CWR, T_6- nawadnianie kropelkowe oparte na czasomierzu do 60% CWR and T_7 - Tradycyjne nawadnianie kropelkowe do 100% CWR, w celu prześledzenia czasowych fluktuacji zawartości wody glebowej przy użyciu modelu numerycznego HYDRUS 2D. Przy użyciu zaobserwowanych danych zastosowano odwrotne rozwiązanie w celu optymalizacji parametrów hydraulicznych wody. Model wykorzystano do przewidzenia zawartości wody glebowej dla siedmiu zabiegów przy optymalnych warunkach. Błąd średniokwadratowy (MSE) oraz pierwiastek błędu średniokwadratowego (RMSE) oraz współczynnik determinacji (R^2) wykorzystano do oceny zgodności pomiędzy wartościami przewidywanymi a danymi. Przy RMSE wynoszącym od 0,036 do 0,067 $cm^3 \cdot cm^{-3}$, MAE od 0,020 do 0,059, oraz R^2 0,848 do 0,959, wyniki pokazują, że model dobrze odzwierciedlił różnice w zawartości wody glebowej we wszystkich miejscach i siedmiu zastosowanych zabiegach.

Słowa kluczowe: Automatyczne nawadnianie kropelkowe, HYDRUS-2D, opcja z folią, zawartość wody w strefie korzeniowej, ruch wody glebowej.